

1
2
3
4
5
6
7
8
9
10
11
12
13
14
15
16
17
18
19
20
21
22
23
24
25
26
27
28
29
30
31
32
33
34
35
36
37
38
39
40
41
42

Heat Shock in *C. elegans* Induces Downstream of Gene Transcription and Accumulation of Double-Stranded RNA

Marko Melnick^{1*}, Patrick Gonzales¹, Joseph Cabral¹, Mary A. Allen², Robin D. Dowell³,
Christopher D. Link^{1,4}

¹ Integrative Physiology, University of Colorado, Boulder, Colorado USA

² BioFrontiers Institute, University of Colorado, Boulder, Colorado USA

³ BioFrontiers Institute and Department of Molecular, Cellular and Developmental Biology, University of Colorado, Boulder, Colorado USA

⁴ Institute for Behavioral Genetics, University of Colorado, Boulder, Colorado, USA

* Corresponding author

E-mail: marko.melnick@colorado.edu

43 **Abstract**

44 We observed that heat shock of *Caenorhabditis elegans* leads to the formation of nuclear
45 double-stranded RNA (dsRNA) foci, detectable with a dsRNA-specific monoclonal antibody.
46 These foci significantly overlap with nuclear HSF-1 granules. To investigate the molecular
47 mechanism(s) underlying dsRNA foci formation, we used RNA-seq to globally characterize total
48 RNA and immunoprecipitated dsRNA from control and heat shocked worms. We find antisense
49 transcripts are generally increased after heat shock, and a subset of both sense and antisense
50 transcripts enriched in the dsRNA pool by heat shock overlap with dsRNA transcripts enriched
51 by deletion of *tdp-1*, which encodes the *C. elegans* ortholog of TDP-43. Interestingly, transcripts
52 involved in translation are over-represented in the dsRNAs induced by either heat shock or
53 deletion of *tdp-1*. Also enriched in the dsRNA transcripts are sequences downstream of
54 annotated genes (DoGs), which we globally quantified with a new algorithm. To validate these
55 observations, we used fluorescence *in situ* hybridization (FISH) to confirm both antisense and
56 downstream of gene transcription for *eif-3.B*, one of the affected loci we identified.

57

58 **Introduction**

59 Cytoplasmic proteotoxic stress induced by temperatures outside of the optimal range for
60 cells or organisms triggers the heat shock response (HSR) [1]. The response to heat shock is
61 multi-faceted and regulation of both transcription and translation occurs. Transcriptional
62 responses include formation of stress granules, alternative splicing, and aberrant transcriptional
63 termination [2–5]. The HSR is a highly conserved transcriptional response and is driven largely
64 by the heat shock transcription factor HSF1 [6]. Under basal level conditions, HSF1 is a
65 monomer in the cytoplasm and nucleus. Upon stress, HSF1 undergoes homotrimerization and
66 binds to DNA heat shock elements (HSE) and initiates the transcription of heat shock protein

67 genes [7,8]. In addition, translation of non-heat shock mRNAs is reduced through pausing of
68 translation elongation as well as inhibition of translation initiation [9–11]. Regulation and
69 clearance of misfolded proteins by heat shock proteins has been implicated in neurodegenerative
70 diseases such as Huntington’s disease (HD), Parkinson’s disease (PD), Alzheimer’s disease
71 (AD), and amyotrophic lateral sclerosis (ALS) [12].

72 Aside from the canonical binding of HSF1 to HSE loci, heat shock can cause HSE-
73 independent transcriptional changes [2]. In mammalian cells, HSF1 granules co-localize with
74 markers of active transcription where HSF1 binds at satellite II and III repeat regions [13]. In the
75 worm *Caenorhabditis elegans*, HSF-1 granules also show markers of active transcription but the
76 putative sites of HSF-1 stress granule binding are unknown [14].

77 In addition to formation of HSF1 stress granules, heat shock can cause reduced efficiency
78 of transcription termination and the accumulation of normally untranscribed sequences,
79 designated in the literature as downstream of gene-containing transcripts (DoGs) [5]. In
80 eukaryote transcriptional termination, the Carboxyl-terminal domain (CTD) of RNA Polymerase
81 II (Pol II) interacts with a complex of cleavage and polyadenylation (CPA) factors responsible
82 for generating the polyadenylate [Poly(A)] tail at mRNA 3’ ends. Two models exist for how the
83 pre-mRNA poly(A) site (PAS) contributes to transcription termination. The allosteric model
84 proposes that Pol II senses PAS during elongation leading to a conformational change in the Pol
85 II active site eventually leading to Pol II release. The other, dubbed the torpedo model, proposes
86 that the nuclear 5’-3’ exonuclease Xrn2 is recruited to the PAS and triggers Pol II release when it
87 degrades the downstream transcript and catches up to elongating Pol II [15].

88 Recent studies have shown increased antisense transcription when DoGs/Read-through
89 transcription goes past the PAS into neighboring genes on opposite strands [16–19]. Antisense

90 transcription has the potential to modulate gene expression by creation of double-stranded RNA
91 (dsRNA) with subsequent degradation through RNA interference (RNAi) [20].

92 Previous studies in our lab found deletion of *tdp-1*, the worm ortholog of ALS associated
93 protein TDP-43, results in the accumulation of dsRNA foci [21]. In addition to deletion of *tdp-1*,
94 we discovered that heat shock robustly induced nuclear dsRNA foci in worms. To assay this
95 unexpected formation of dsRNA, we performed strand-specific RNA-seq and strand-specific
96 RNA-immunoprecipitation sequencing (RIP-seq) with the J2 antibody specific for dsRNA. In
97 heat shocked worms, we find increased J2 enrichment of downstream-of-gene transcripts as well
98 as genes involved in translation. To identify altered transcription genome-wide, we developed an
99 algorithm called Dogcatcher that provides DoG locations, differential expression of DoGs, and
100 genes that overlap with DoGs on the same or opposite strand.

101

102 **Materials and Methods**

103

104 ***Caenorhabditis elegans* culturing and strains**

105 Hermaphrodites from each strain were kept at 16 °C on Nematode Growth Media (NGM)
106 plates seeded with *Escherichia coli* strain OP50 as a food source according to standard practices
107 [22]. To obtain age synchronized worms, we used alkaline hypochlorite bleach on gravid adults
108 to obtain eggs that were hatched overnight in S-basal buffer [23]. Worms were then allowed to
109 grow to 1-day-old adults (approximately 80h at 16 °C). List of strains used in this study is
110 available in S1 Table.

111

112 **Heat stress treatment**

113 Heat stress treatment was performed in an air incubator set to 35 °C for 3 hours for the
114 RNA-seq experiments. After stress, populations were washed off with S-basal buffer and
115 immediately fixed for immunohistochemistry and/or fluorescence in situ hybridization (FISH),
116 flash frozen in liquid nitrogen for quantitative reverse transcriptase polymerase chain reaction
117 (qRT-PCR), or crude extracts were created with subsequent J2-Immunoprecipitation (J2-IP) as
118 previously described [21].

119

120 **RNA isolation, cDNA library preparation, and RNA Sequencing**

121 Total RNA was extracted from worms using TRIzol (Invitrogen #15596026) extraction.
122 Chloroform was used to solubilize proteins and TURBO DNase (Invitrogen) was used to remove
123 DNA. For total RNA libraries, 5 µg of RNA was ran through a RiboZero column (Epicenter,
124 #R2C1046) to remove ribosomal RNA. Libraries were created using Illumina TruSeq kits (RS-
125 122-2001). RNA recovered by immunoprecipitation with the J2 antibody of young adult worms
126 as well as input material (as a loading control) was converted into strand-specific total RNA
127 libraries using V2 Scriptseq (Epicenter #SSV21106) kits following manufacturer's instructions,
128 except reverse transcription was done with SuperScript III (Invitrogen #18080 044) using
129 incrementally increasing temperatures from 42 to 59 °C to allow for transcription though
130 structured RNAs. rRNA was not removed from J2-IP RNA samples. Libraries were sequenced
131 on an Illumina HiSeq 2000 platform at the Genomics Core at the University of Colorado,
132 Denver. Data were deposited under GEO accession number GSE120949.

133

134 **Immunohistochemistry and Fluorescence in situ Hybridization**

135 **(FISH)**

136 For immunohistochemistry, all washes used a constant volume of 1ml sterile S-basal
137 buffer unless otherwise noted. Worms were first washed off plates, spun down into a pellet, and
138 fixed in 4% paraformaldehyde. Worms were then resuspended in 1ml of Tris/Triton buffer with
139 5% beta-mercaptoethanol and incubated in a rocker for two days at 37°C. After two days, worms
140 were washed two times and put into collagenase buffer. Next, worms were placed into a 1:1
141 dilution of 1mg/ml type IV collagenase (Sigma) and S-basal buffer for 45 minutes at 37 °C with
142 rocking. Worms were checked under the microscope to ensure cuticle breakage then quenched in
143 cold Antibody buffer A (1X Phosphate buffered saline, 0.1% Bovine Serum Albumin, 0.5%
144 Triton X-100, 0.05% Sodium Azide). Worms were then washed, pelleted, and primary antibodies
145 were added for 16 hours at 4°C. Next, worms were washed twice in Antibody buffer B (same as
146 Antibody buffer A except using 1% Bovine Serum Albumin), pelleted, and secondary antibodies
147 were added with subsequent incubation for 2 hours at room temperature. Finally, worms were
148 washed twice in Antibody buffer B and then placed in 50/mul of Antibody buffer A.

149 Permeabilized worms were probed with the primary J2 antibody (English and Scientific
150 Consulting Lot: J2-1102 and J2-1103) at 4µg/mL and secondary antibody Alexa dye-conjugated
151 goat anti-mouse at 4µg/mL. DAPI nuclear stain was added along with secondary antibodies at
152 5µg/mL to visualize nuclei.

153 Stellaris FISH probes (Biosearch technologies) [24] were custom designed using the
154 Stellaris RNA FISH probe designer. Three regions were chosen for probing, and each probe was
155 tested against the *C. elegans* genome using BLAST to identify any complementarity to non-
156 target sequences. A probe was excluded if it was in an intron, had a highly repetitive sequence

157 outside of the region, or matched other regions up to 18nt long with high transcriptomic
158 expression viewed in the Integrative Genome Viewer (IGV) [25] Probes and locations are
159 available in S1 File.

160 For FISH probing and storage, the Stellaris protocol for *C. elegans* was followed using
161 RNAase OUT (Invitrogen) when applicable. Briefly, worms were washed off plates using
162 nuclease-free water and fixed for 45 minutes at room temperature in a fixation buffer (1:1:8 of
163 37% Formaldehyde, 10X RNase-free Phosphate Buffered Saline (PBS), Nuclease-free water).
164 Worms were then washed twice with 1X RNAase-free PBS and permeabilized in 70% ethanol
165 overnight at 4°C. Worms were then incubated at room temperature in Stellaris Wash Buffer A,
166 pelleted, and incubated for 16 hours in a 37 °C water bath in the dark with 100µl of the
167 probe/hybridization buffer (9:1 of µl Stellaris RNA FISH Hybridization buffer, Deionized
168 Formamide with a 100:1 Hybridization buffer, FISH probe). Next, 1mL of Stellaris Wash Buffer
169 A was added with 30 more minutes of incubation in the dark 37 °C water bath. Stellaris Wash
170 Buffer A was then aspirated and incubated with DAPI (1:1000 of 5µg/m DAPI, Stellaris Wash
171 Buffer A) for 30 more minutes of the dark 37 °C water bath. Lastly, the DAPI buffer was
172 aspirated and 1mL of Stellaris Wash Buffer B was added with a 5 minutes room temperature
173 incubation.

174 A modification of the immunohistochemistry protocol was used when doing
175 immunohistochemistry and FISH. The immunohistochemistry protocol was the same except all
176 washes were done using RNAase-free PBS or water and RNAase-free reagents (Tris/Triton
177 Buffer, Collagenase Buffer, Collagenase, Antibody Buffer A, Antibody Buffer B) were created
178 by adding RNAase OUT (2:10000 of RNAase OUT, reagent). After antibody staining, the FISH
179 protocol was started at the probe/hybridization step.

180

181 **Microscopy**

182 Images were acquired with a Zeiss Axiophot microscope equipped with digital deconvolution
183 optics (Intelligent Imaging Innovations). Image brightness and contrast were digitally adjusted in
184 Photoshop.

185

186 **Quantification of occurrence of HSF-1 and J2 foci over time**

187 Intestinal nuclei of the worms were isolated from the rest of the image and the Foci Picker3D
188 plug-in was used to count foci. The FITC channel of the image was converted to 16 bit and
189 analyzed. Foci Picker3D settings were changed from default by changing the MinIsetting to 0.25
190 and the ToleranceSetting to 20 before running analysis. Five worms were selected for each time
191 point. Raw data is available in S2 Table.

192

193 **Data Analysis**

194 Detailed instructions on algorithms and analysis is provided in S3 file. Briefly, reads
195 were checked for quality with FastQC v0.11.7 [26], adapters were trimmed using Trimmomatic-
196 0.36 [27] (S2 file), and reads were aligned to the worm genome WS258 using STAR-2.5.2b [28].
197 Genes and DoGs (identified by Dogcatcher, described below) were assigned counts using
198 Rsubread v1.28.1 featureCounts [29] and were rRNA-normalized according to the rRNA
199 subtraction ratio (RSR) (described in supplemental). Differential expression was obtained using
200 DESeq2 v1.20.0 and the likelihood ratio test (LRT) set with Total/Input and J2 treated as
201 separate variables within the condition [30].

202 We created an algorithm called Dogcatcher to identify and analyze DoGs. Briefly,
203 Dogcatcher uses a sliding window approach to identify contiguous regions of transcription above
204 a defined threshold. If the sliding window runs into a gene on the same strand it will either
205 continue (meta read-through) or stop (local read-through). Dogcatcher will output bedfiles, gtf's
206 and dataframes of all DoGs and antisense DoGs for a sample along with differential expression
207 and genes overlapping DoGs (For additional details see bioinformatics supplemental S3 File).
208 For improved normalization in DESeq2, non-significant genes are added when calculating
209 differential expression and removed afterward. The Dogcatcher algorithm and README is
210 available at <https://github.com/Senorelegans/Dogcatcher>. For processing J2 enrichment, a
211 modified version of Dogcatcher was used that applies the rRNA subtraction ratio normalization
212 and likelihood ratio test from DESeq2 (available at
213 [https://github.com/Senorelegans/heatshock_and_tdp-](https://github.com/Senorelegans/heatshock_and_tdp-1_dsRNA_scripts/J2_enrichment_Dogcatcher)
214 [1_dsRNA_scripts/J2_enrichment_Dogcatcher](https://github.com/Senorelegans/heatshock_and_tdp-1_dsRNA_scripts/J2_enrichment_Dogcatcher)).
215 After Dogcatcher was used, DoGs overlapping operons on the same strand were removed (S3
216 File for operon removal methods).
217 All of the scripts used to process the data and create figures can be found at
218 https://github.com/Dogcatcher/heatshock_and_tdp-1_dsRNA_scripts

219

220 **Results**

221

222 **Heat shock induces nuclear dsRNA foci in *C. elegans***

223 While looking for conditions that might induce dsRNA foci besides loss of *tdp-1*, we

224 found that heat shock robustly induced dsRNA nuclear foci. Upshifting wild type worms to 35

225 °C or 37 °C induced foci detectable with the J2 dsRNA-specific monoclonal antibody within 30
226 minutes, primarily visible in intestinal and hypodermal nuclei. To determine if these foci
227 overlapped with previously identified nuclear HSF-1 stress granules, we repeated the heat shock
228 experiment with strain OG497 (*drSI13*) [14]. This strain has a single copy insertion of *hsf-1* with
229 a C-terminal GFP driven by the *hsf-1* promoter, and shows nuclear GFP expression that
230 redistributes into granules after a one minute heat shock at 35 °C [14]. Using the J2 antibody for
231 immunohistochemistry, we found J2 dsRNA foci in nuclear regions that partially overlapped
232 with nuclear HSF-1 stress granules when *drSI-13* worms were heat shocked for 35 °C for 40
233 minutes (Fig 1).

234 **Fig 1. Heat shock induces nuclear foci detectable with dsRNA-specific antibody J2.**
235 (A) Mid-animal intestinal region of 4th larval stage *drSI13* worm fixed 40 minutes after heat
236 shock at 35° C. Note nuclear J2 foci (orange arrows), many of which overlap with HSF-1 foci.
237 HSF-1-only foci indicated by green arrows. White size bar in bottom right corner (20 microns
238 across). (B) Quantification of occurrence of HSF-1 and J2 foci over time, 4 intestinal nuclei per
239 worm scored.
240

241 **Recovery of dsRNA by J2 immunoprecipitation**

242 In order to identify dsRNA transcripts induced by heat shock, we performed strand
243 specific RNA sequencing (RNA-seq) and strand specific RNA immunoprecipitation sequencing
244 (RIP-seq) (Fig 2). Total/Input RNA and RNA immunoprecipitated with the J2 antibody was
245 extracted and sequenced for heat shocked N2 (wild type) worms (in duplicate) and non-heat
246 shocked worms (in triplicate). The J2 antibody is specific for dsRNA 40bp or more [31].
247 Importantly, transcripts from the J2 IP could include full length dsRNA transcripts or single
248 stranded RNA (ssRNA) with 40bp or more sections of dsRNA. dsRNA can occur via base
249 pairing with a different transcript (interstrand) or self-complementarity within the same transcript
250 (intrastrand).

251 **Fig 2. Schematic of recovery of RNA pools for high throughput sequencing analysis.**

252 Control and heat shocked worm populations were recovered and lysed. Worm lysates were then
253 split to recover total input RNA or immunoprecipitated with the J2 antibody.
254

255 **Antisense transcripts increase after heat shock**

256
257 The apparent increase in dsRNA we observed in heat shocked worms [and previously
258 observed in the *tdp-1(ok803)* mutant] could result from an increased accumulation of antisense
259 transcripts. To obtain a global view of antisense levels, we calculated an antisense/sense ratio for
260 genes using the total RNA samples (S3 File for methods). Genes with a minimum of 20 antisense
261 and 20 sense reads were used for the analysis. For both heat shock and *tdp-1(ok803)* samples, we
262 found a strong trend towards increased antisense/sense ratios compared to normal conditions (Fig
263 3). Heat shock results in 77% of the genes tested (785/1016) having increased antisense/sense
264 ratios > 1 compared to wild type, and *tdp-1(ok803)* having 86% (799/925) with increased ratios
265 compared to wild type. Notably, heat shock produced a higher average antisense/sense ratio with
266 a greater spread of ratios compared to *tdp-1(ok803)*.

267 **Fig 3. Quantification of genes with changes in antisense/sense ratios after heat shock or deletion of**
268 ***tdp-1* in total RNA.** 785 genes up in antisense and 231 genes down in antisense for heat shock (HS)
269 compared to wild type (WT) using the ratio of antisense/sense. 799 genes up in antisense and 126 genes
270 down in antisense for *tdp-1(ok803)* using the ratio of antisense/sense. Colored dots represent genes with
271 increased antisense (green) and decreased antisense (blue) compared to wild type (n=1).
272

273 **Comparison of dsRNAs identified in worms heat shocked or deleted**
274 **for *tdp-1***

275 Considering that both heat shock and deletion of the *tdp-1* gene lead to the formation of
276 nuclear dsRNA foci, we sought to determine if this phenotypic similarity also extends to
277 transcriptional changes. After heat shock, we found that a large number of gene transcripts were
278 significantly (FDR <0.05) enriched (4774) or depleted (1669) in the pool of RNAs

279 immunoprecipitated by the dsRNA-specific antibody J2 (relative to untreated worms) (Fig 4A).
280 We also identified antisense transcripts with significantly altered representation in the J2-
281 immunoprecipitated pool, and found 650 were enriched and 477 depleted (Fig 4B). A minority of
282 genes had both sense and antisense transcripts significantly enriched (180) or depleted (48) in the
283 heat shock J2-IP pool (Fig 4A-B) (plot of genes showing only significant sense and antisense
284 transcription for heat shocked worms in S1 Fig). In *tdp-1(ok803)* significant (FDR <0.05) gene
285 transcripts, we found a smaller number of sense enriched (418) and depleted (59) (Fig 4C), as
286 well as antisense enriched (245) and depleted (14) genes (Fig 4D). Similar to heat shock, *tdp-*
287 *1(ok803)* had relatively fewer genes with both sense and antisense transcripts significantly
288 enriched (6) and depleted (1) (Fig 4C-D) (plot of genes showing only significant sense and
289 antisense transcription for *tdp-1(ok803)* worms in S2 Fig). We found a significant [$P < 1 \times e^{-30}$,
290 hypergeometric (hgd)] overlap of J2-enriched gene transcripts between the heat shock and *tdp-*
291 *1(ok803)* populations in both sense (Fig4 E) and antisense (Fig4 F), suggesting that there might
292 be some similarities between the transcriptional changes induced by heat shock and deletion of
293 *tdp-1*. However, with J2-depleted transcripts, we found no significant overlap in ($P = 0.165$,
294 hgd) in sense transcripts and no significant overlap in antisense transcripts ($P = 0.187$, hgd) (See
295 supplemental S4 File for list of genes and hgd implementation).

296 **Fig 4. Comparison of J2 enriched sense and antisense transcripts in heat shock and *tdp-***
297 ***1(ok803)* worms.**

298 MA plots of significant (FDR <0.05) dsRNA enrichment for sense and antisense transcripts (analyzed
299 independently) along with Venn diagrams of enrichment for enriched sense and antisense. (A) Heat shock
300 over wild type J2 enriched sense transcripts with 4774 enriched (red) and 1669 depleted (blue). (B) Heat
301 shock over wild type J2 enriched antisense transcripts with 650 enriched (red) and 477 depleted (blue).
302 (A-B) enriched (180) and depleted (48) heat shock vs wild type transcripts found in both sense and
303 antisense (green triangles). C: *tdp-1(ok803)* over wild type significant J2 enriched sense transcripts with
304 418 enriched (purple) and 59 depleted (blue). (D) *tdp-1(ok803)* over wild type significant J2 enriched
305 antisense transcripts with 245 enriched (purple) and 14 depleted (blue). (C-D) enriched (6) and depleted
306 (1) *tdp-1(ok803)* vs wild type transcripts found in both sense and antisense (green triangles). (E) Overlap
307 of genes with significantly J2 enriched sense transcripts in both conditions compared to wild type worms.

308 (F) Overlap of genes with significantly J2 enriched antisense transcripts in both conditions compared to
309 wild type worms.
310

311
312 We used gene ontology (GO) analysis to investigate if transcripts enriched in the J2
313 immunoprecipitation fell into any functional categories. Using GOATOOLS [32], we found that
314 many GO terms related to translation were significantly enriched (FDR < 0.05) in both the heat
315 shock and *tdp-1(ok803)* J2-IP pools. In order to get the total number of genes involved in
316 translation, which we call “translation related genes”, we combined lists of genes from all
317 significantly enriched GO terms containing the words “translation”, “ribosome”, and
318 “ribosomal”, then removed duplicate genes that were members of multiple GO terms (S3 File for
319 methods). In sense J2 enriched transcripts, we find 234 translation related genes with heat shock,
320 27 translation related genes in *tdp-1(ok803)*, and 19 translation related genes in the overlap. In
321 the J2 depleted sense pool, heat shock contained 30 translation related genes, *tdp-1(ok803)*
322 worms had no translation related genes, as well as no translation related genes in the overlap. In
323 J2-enriched antisense transcripts, only heat shocked worms had 33 translation related genes.
324 There was no translation related genes found in J2-depleted antisense transcripts (S5 File for list
325 of significant genes and translation related genes, S6 File for GOATOOLS output).

326

327

328 **Enrichment of transcripts downstream of genes in the J2 pool**

329 While examining the transcription of known heat shock-inducible genes, we noted in heat
330 shocked populations an accumulation of read-through transcripts downstream of annotated genes
331 (see example in Fig 5). Interestingly, some of these downstream-of-gene transcripts (DoGs)
332 were also highly enriched in the J2-IP pool. While previous work has characterized the

333 accumulation of downstream-of-gene transcripts in heat shocked cells from human [5] and mice
334 [16], the phenomena has not previously been associated with dsRNA accumulation. To assay and
335 find differential expression of these read-through regions across the whole genome, we created
336 an algorithm called Dogcatcher (See methods and materials as well as GitHub README for
337 algorithm explanation).

338
339
340 **Fig 5. Aberrant transcription past the end of heat shock family genes showed enrichment in heat**
341 **shock J2.**
342 Ribosomal subtracted ratio normalized histogram from the Integrative Genomics Viewer (IGV). On each
343 track, the sense strand is on the top part of the histogram and antisense is on the bottom. Wild type (WT)
344 sense (dark blue) and antisense (light blue), heat shock (HS) sense (red) and antisense (orange).
345 Downstream of gene transcription (DoG) continues past the 3' end of gene (green arrow).
346

347
348 Using the Dogcatcher algorithm, we were able to quantify downstream-of-gene
349 transcripts in the J2 -IP pool that can be missed using the standard *C. elegans* genome
350 annotation. After heat shock, more read-through sections were significantly increased in the J2-
351 IP pool than decreased (84 vs. 25). (Fig 6A). We found that for DoGs enriched in the J2-IP pool
352 after heat shock, the majority correspond to protein coding genes (60%), followed by ncRNA
353 (20%), pseudogenes (9%), and snoRNA (9%). We found far fewer significantly J2 enriched
354 DoGs from *tdp-1(ok803)* (3) with no regions being depleted (Fig 6B). Interestingly, 2 out of the
355 3 DoGs in *tdp-1(ok803)* were also enriched in the heat shock J2 pool (S4 File for list DoGs and
356 hgd implementation). From the significantly enriched GO terms of DoGs in heat shock and *tdp-*
357 *1(ok803)* worms, only heat shocked worms had any significantly enriched GO terms which
358 primarily consisted of histone genes (S7 File for list of DoGs, S8 File for GOATOOLS output).
359 As a possible explanation for the formation of dsRNA at downstream of gene regions, we found
360 DoGs to be enriched in terminal repeat sequences compared to a random intergenic downstream
361 background. (S3 Fig, S3 File for methods).

362 **Fig 6. J2 enrichment of DoGs and ADoGs in heat shock and *tdp-1(ok803)* worms.**

363 MA plots of significant (FDR <0.05) dsRNA enrichment for DoGs and ADoGs. Non-significant genes
364 added in with DoGs/ADoGs for DESeq2 normalization were taken out of the plots for clarity. (A) heat
365 shock over wild type J2 enriched read-through sense transcripts with 84 enriched (red) and 25 depleted
366 (blue). (B) *tdp-1(ok803)* over wild type significant J2 enriched read-through sense transcripts with 3
367 enriched (purple). (C) heat shock over wild type J2 enriched read-through antisense transcripts with 2
368 enriched (red). (D) No significant *tdp-1(ok803)* over wild type J2 enriched read-through antisense
369 transcripts.

370

371 **Additional non-annotated transcripts are minimally enriched in the**

372 **J2 pool after heat shock or *tdp-1* deletion**

373 Next, we were curious if other sections around genes would show aberrant transcription
374 in heat shock or *tdp-1(ok803)* worms. Expanding on the DoG nomenclature, the terms we use for
375 the three other types of transcription flanking an annotated gene are as follows. Regions
376 downstream of genes with antisense reads (ADoGs), sense reads in regions upstream/previous of
377 the gene (POGs), and antisense reads in regions upstream/previous of the gene (APOGs) (See S4
378 Fig for visualizations and additional explanation). Importantly, novel areas of intergenic
379 transcription are obtained by filtering out POGs that overlap with DoGs on the same strand, as
380 well as ADoGs/APOGs that overlap DoGs or genes on the opposite strand (See S5 Fig for
381 visualization of filtering). We did not find any significantly J2 enriched POGs or APOGs in
382 either condition compared to wild type. We found a small amount of significant J2 enrichment in
383 heat shock ADoGs (2) (Fig 6C) and no ADoGs enriched in *tdp-1(ok803)* (Fig 6D).

384 **Increased antisense transcription over genes associated with DoGS**

385 **and ADoGS**

386 Next, we were curious if any aberrant read-through transcription might overlap genes and
387 contribute to increased antisense reads within the gene. We define an overlapped gene as any
388 gene that has an ADoG associated with it or an opposite strand DoG with any overlap to the
389 gene. We next define a significant overlapped gene as any gene that has significant antisense
390 transcription as well as a significant ADoG or significant DoG that overlaps it on the opposite
391 strand. From our significantly overlapped genes, we found 17 enriched and 5 depleted with heat
392 shock, and only 4 enriched and no depleted in *tdp-1(ok803)* worms. We did not find any
393 overlapped genes that were significantly enriched for GO terms related to translation (S5 File for
394 list of overlapped genes, S3 File for overlap methods).

395
396

397 **Antisense read-through into *eif-3.B* in heat shocked worms**

398 Visual inspection of DoG transcripts identified one transcript downstream of the ncRNA
399 *W01D2.8* (*doW01D2.8*) that ran into the gene *eif-3.B* on the opposite strand. (Fig 7A). *eif-3.B* is
400 an ortholog of human EIF-3.B (eukaryotic translation initiation factor 3 subunit B) and is
401 involved in translation initiation. As the *doW01D2.8* transcript was strongly increased by heat
402 shock in both the total and J2-IP pools, we chose to target this transcript to confirm our RNA-seq
403 data. Fluorescent *in situ* hybridization (FISH) was used as this could both demonstrate the
404 accumulation of the *doW01D2.8* transcript and determine its cellular and subcellular (i.e.,
405 possible co-localization with J2 foci) distribution.

406 **Fig 7. Heat shock induces transcripts antisense to the *eif-3B* locus.**

407 IGV view of *eif-3.B*. Tracks normalized by the ribosomal subtraction ratio, the sense strand is on the top
408 part of the histogram and antisense is on the bottom. wild type (WT) sense (dark blue), WT antisense
409 (light blue), heat shock sense (red), heat shock antisense (orange). Horizontal red arrows on the right
410 show a cluster of ncRNAs including *W01D2.8* and transcription downstream of *W01D2.8* (*doW01D2.8*)
411 into *eif-3.B* (green arrow going left). Arrows on the bottom correspond to locations of primers for RT-
412 PCR (brown: 5' Intergenic, purple: Second exon, black: 3' UTR).

413
414 Three strand-specific fish probes at the 5' Intergenic region (5' INT) (antisense), first 3
415 exons (sense), and the last exon along with the 3' UTR (LE 3'UTR) (antisense) of *eif-3.B* (Fig
416 8D) were designed (list of probes in S1 File). First, we performed immunohistochemistry with
417 the J2 antibody along with FISH for antisense transcripts that contain the last exon and 3' UTR
418 (see Material and Methods) (Fig 8A). We find that *doW01D2.8* is transcribed in this region with
419 heat shock and commonly forms two foci per nucleus, but does not co-localize with dsRNA foci.
420 The 5' and 3' *doW01D2.8* probes do strongly colocalize in the nuclear foci (Fig 8B), consistent
421 with a single transcript spanning this region. Additionally, when probing for the 5' intergenic
422 region (antisense) and first three exons (sense), we did not find the sense probes colocalizing to
423 the antisense foci (S6 Fig). To inquire if the *eif-3B* antisense foci were a general site of transcript
424 accumulation, we probed for *C30E1.9*, a long ncRNA that is highly expressed, forms nuclear
425 foci, but is not induced in heat shock. We observed that this transcript does not overlap with the
426 *eif-3B* antisense foci (Fig 8C). Lastly, we wanted to see if deletion of *tdp-1*, which does not lead
427 to accumulation of *eif-3B* antisense transcripts, would alter heat shock induced accumulation of
428 these transcripts. We found that the *tdp-1* deletion did not alter the formation of *eif-3B* antisense
429 transcripts (Fig 8E).

430 **Fig 8. Fluorescence in situ Hybridization (FISH) of *eif-3.B* regions.**

431 100x oil immersion images of worm hypodermal and neuronal cells. Heat shock panels are in the three
432 columns to the left (merged channel in the middle column). Control panels show exposure from every
433 channel (right column). Row (A) Immunohistochemistry with J2 antibody (green) along with FISH of
434 *doW01D2.8* antisense to the last exon and 3' UTR (LE 3' UTR) (red) of *eif-3.B*. dsRNA and the antisense
435 LE 3'UTR transcript aggregate into nuclear foci with heat shock and do not appear to co-localize. Row
436 (B) FISH of *doW01D2.8* in two regions antisense to the 5' intergenic region (5' INT) (green) and last
437 exon and 3' UTR (LE 3'UTR) (red) of *eif-3.B*. Row (C) FISH of *doW01D2.8* antisense to the last exon
438 and 3' UTR (LE 3'UTR) (red) of *eif-3.B* and sense probe of ncRNA C3DE1.9 (green). Probing of
439 C3DE1.9 is not affected by heat shock and C3DE1.9 is not induced by heat shock. C3DE1.9 and LE
440 3'UTR show no overlap. (D) Diagram of *eif-3.b* gene with FISH probe locations and orientation. (E) Heat
441 shock of *tdp-1(ok803)* induces nuclear foci from probes antisense to the last exon and 3' UTR (LE

442 3'UTR) of *eif-3.B* (left panel) and is not visible with no heat shock (right).

443

444 **Discussion**

445

446 In our previous study [21] we established that in *C. elegans* deletion of *tdp-1* induces
447 nuclear dsRNA foci. Here, we show that heat shock also induces nuclear dsRNA foci that
448 partially overlap with HSF-1 nuclear stress granules. After heat shock, we find a general increase
449 in the amount of dsRNA and expression levels of transcripts with dsRNA structure, assayed
450 using the dsRNA-specific monoclonal antibody J2. In addition, we find that heat shock induces
451 accumulation of antisense transcripts as well as novel downstream of gene transcripts. To our
452 knowledge this is the first time heat shock has been shown to lead to the accumulation of these
453 abnormal transcripts in an *in vivo* model.

454 dsRNA can form intra- or inter- strand base-pairing. Our data suggest that both types of
455 dsRNA may be contributing to the dsRNA pool induced by heat shock. We find that novel
456 downstream-of-gene transcripts are enriched in the J2-IP pool. These novel transcripts are
457 enriched in inverted repeat sequences, which may be contributing to the formation of intra-strand
458 dsRNA. Downstream-of gene transcripts also have the potential to generate transcripts antisense
459 to neighboring genes on the other strand. This has been reported in the heat shock study by
460 Vilborg et al [16], and we have noted similar examples in our data (see Figure 8). Using our new
461 Dogcatcher algorithm, we have also documented novel transcripts originating in intergenic
462 regions, which also have the potential to generate antisense transcripts. Indeed, we observe a
463 general increase in antisense transcription after heat shock (see Figure 3), and antisense
464 transcripts are enriched in the J2-IP, supporting the formation of inter-strand dsRNA. We note
465 that the J2 antibody immunoprecipitation protocol used in our study will recover transcripts that

466 have only partial (at least 40 nucleotides) dsRNA structure, thus it is feasible that some
467 transcriptional regions we recover after J2-IP are single-stranded extensions of double stranded
468 regions.

469 The accumulation of dsRNA transcripts after heat shock could be the result of altered
470 RNA production and/or changes in RNA stability or turnover. Further studies (e.g. Pro-seq
471 analysis) will be required to definitively determine the relative contribution of these cellular
472 processes. Published studies demonstrate that loci susceptible to heat shock-induced
473 downstream-of-gene transcription are marked by open chromatin before heat shock [16] and are
474 depleted of the transcriptional termination factor CPSF-73 after heat shock [33]. These results
475 suggest that altered transcriptional processing itself leads to the altered transcript accumulation
476 after heat shock. However, the significant overlap of transcripts enriched in the J2 pool resulting
477 from heat shock and from deletion of the *tdp-1* gene suggest that changes in RNA stability may
478 be also contributing to transcript accumulation. TDP-1 is orthologous to mammalian TDP-43,
479 and we have previously shown that human TDP-43 can act as an RNA chaperone in an *in vitro*
480 assay [21]. Conceivably, heat shock could inhibit the function of TDP-1 or other similar RNA-
481 binding proteins, leading to the formation of more dsRNA structure in existing transcripts.

482 We employed fluorescence in situ hybridization (FISH) to confirm heat shock-induced
483 expression of DoG and antisense transcripts in the *eif-3.B* region, and to examine their sub-
484 cellular localization. These novel transcripts were found in nuclear foci that did not overlap with
485 either the HSF-1::GFP foci or the J2 dsRNA foci, and were typically limited to two spots in each
486 nuclei. This two foci/nucleus distribution is very similar to the FISH characterization of DoG
487 transcripts described by Vilborg et al, and strongly suggest that the *eif-3.B* loci transcripts are
488 associated in *cis* with their site of production. These antisense transcripts clearly did not

489 contribute to the foci detected by J2 immunostaining, and may reflect a general dysregulation of
490 transcription at the *eif-3.B* locus. Identification of the dsRNA species present in the J2 foci
491 induced by heat shock may require development of a protocol to purify these RNA granules, as
492 we have identified thousands of transcripts enriched in the J2 pool, and have no additional
493 insight as to which ones might be found specifically in the J2 foci.

494 A critical issue is whether the accumulation of novel transcripts and dsRNA after heat
495 shock have a biological function. By characterizing transcriptional changes induced by a variety
496 of stresses, Vilborg et al concluded that transcriptional read-through was not a random failure,
497 and suggested it might have a functional role in stress responses. We have characterized the
498 accumulation of dsRNA after heat shock, and by gene ontology analysis find that the sense and
499 antisense transcripts in this pool (as well as the J2-IP pool in *tdp-1* deletion mutants) are enriched
500 in genes involved in translation. Given that we find significant J2-IP enrichment of both sense
501 and antisense transcripts from genes related to translation, it is tempting to speculate that the
502 formation of inter-strand dsRNA might reduce the translation of these “translation-related
503 transcripts”, leading to a down-regulation of global translation, a protective event against most
504 cellular stress insults including heat shock. While we have no direct evidence that dsRNA-
505 dependent translational downregulation happens after heat shock in *C. elegans*, we note that
506 deletion of *tdp-1* has been reported to protect against proteotoxicity and increase lifespan [34].
507 Translational downregulation would presumably be protective against proteotoxicity, and post-
508 developmental knockdown of translation initiation factors strongly increases lifespan in *C.*
509 *elegans* [35].

510 **Acknowledgements**

511 We would like to thank Anna Vilborg for supplying the perl scripts from her initial DoG
512 publication [5]. Some nematode strains were provided by the Caenorhabditis Genetics Center,
513 funded by the NIH National Center for Research Resources.

514
515

516 **References**

- 517
- 518 1. Lindquist S. The Heat-Shock Response. *Annu Rev Biochem. Annual Reviews* 4139 El
519 Camino Way, P.O. Box 10139, Palo Alto, CA 94303-0139, USA; 1986;55: 1151–1191.
520 doi:10.1146/annurev.bi.55.070186.005443
 - 521 2. Gomez-Pastor R, Burchfiel ET, Thiele DJ. Regulation of heat shock transcription factors
522 and their roles in physiology and disease. *Nat Rev Mol Cell Biol. Nature Publishing*
523 *Group*; 2018;19: 4–19. doi:10.1038/nrm.2017.73
 - 524 3. Brewer-Jensen P, Wilson CB, Abernethy J, Mollison L, Card S, Searles LL. Suppressor of
525 sable [Su(s)] and Wdr82 down-regulate RNA from heat-shock-inducible repetitive
526 elements by a mechanism that involves transcription termination. *RNA. 2016;22: 139–54.*
527 doi:10.1261/ma.048819.114
 - 528 4. Shalgi R, Hurt JA, Lindquist S, Burge CB. Widespread inhibition of posttranscriptional
529 splicing shapes the cellular transcriptome following heat shock. *Cell Rep. The Authors*;
530 2014;7: 1362–1370. doi:10.1016/j.celrep.2014.04.044
 - 531 5. Vilborg A, Passarelli MC, Yario TA, Tycowski KT, Steitz JA. Widespread Inducible
532 Transcription Downstream of Human Genes. *Mol Cell. 2015;59: 449–461.*
533 doi:10.1016/j.molcel.2015.06.016
 - 534 6. Gidalevitz T, Prahlad V, Morimoto RI. The stress of protein misfolding: From single cells
535 to multicellular organisms. *Cold Spring Harb Perspect Biol. 2011;3: 1–18.*
536 doi:10.1101/cshperspect.a009704
 - 537 7. Westwood JT, Clos J, Wu C. Stress-induced oligomerization and chromosomal
538 relocalization of heat-shock factor. *Nature. 1991;353: 822–827. doi:10.1038/353822a0*
 - 539 8. Åkerfelt M, Morimoto RI, Sistonen L. Heat shock factors: Integrators of cell stress,
540 development and lifespan [Internet]. *Nature Reviews Molecular Cell Biology. NIH Public*
541 *Access*; 2010. pp. 545–555. doi:10.1038/nrm2938
 - 542 9. Lindquist S. Regulation of protein synthesis during heat shock. *Nature. Nature Publishing*
543 *Group*; 1981;293: 311–314. doi:10.1038/293311a0
 - 544 10. Shalgi R, Hurt JA, Krykbaeva I, Taipale M, Lindquist S, Burge CB. Widespread
545 Regulation of Translation by Elongation Pausing in Heat Shock. *Mol Cell. 2013;49: 439–*
546 *452. doi:10.1016/j.molcel.2012.11.028*
 - 547 11. Sonenberg N, Hinnebusch AG. Regulation of Translation Initiation in Eukaryotes:
548 Mechanisms and Biological Targets [Internet]. *Cell. 2009. pp. 731–745.*
549 doi:10.1016/j.cell.2009.01.042
 - 550 12. Smith HL, Li W, Cheetham ME. Molecular chaperones and neuronal proteostasis. *Semin*
551 *Cell Dev Biol. 2015;40: 142–152. doi:10.1016/j.semcdb.2015.03.003*
 - 552 13. Jolly C, Metz A, Govin J, Vigneron M, Turner BM, Khochbin S, et al. Stress-induced
553 transcription of satellite III repeats. *J Cell Biol. 2004;164: 25–33.*
554 doi:10.1083/jcb.200306104
 - 555 14. Morton EA, Lamitina T. *Caenorhabditis elegans* HSF-1 is an essential nuclear protein that
556 forms stress granule-like structures following heat shock. *Aging Cell. 2013;12: 112–120.*
557 doi:10.1111/accel.12024
 - 558 15. Proudfoot NJ. Transcriptional termination in mammals: Stopping the RNA polymerase II

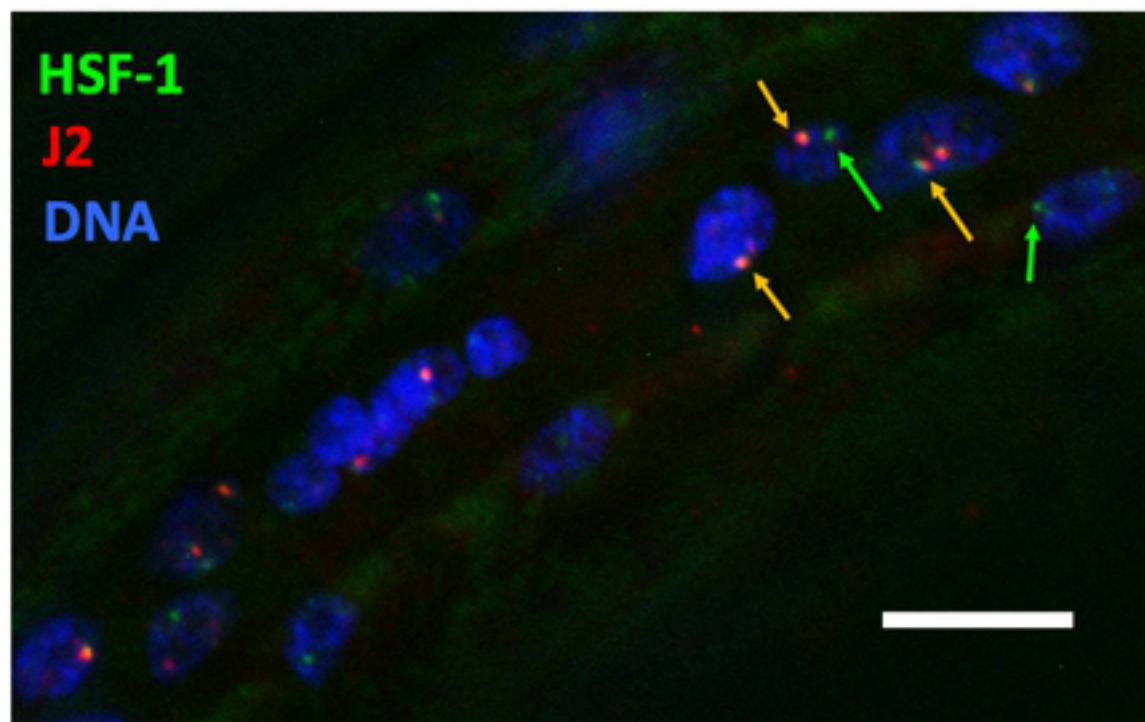
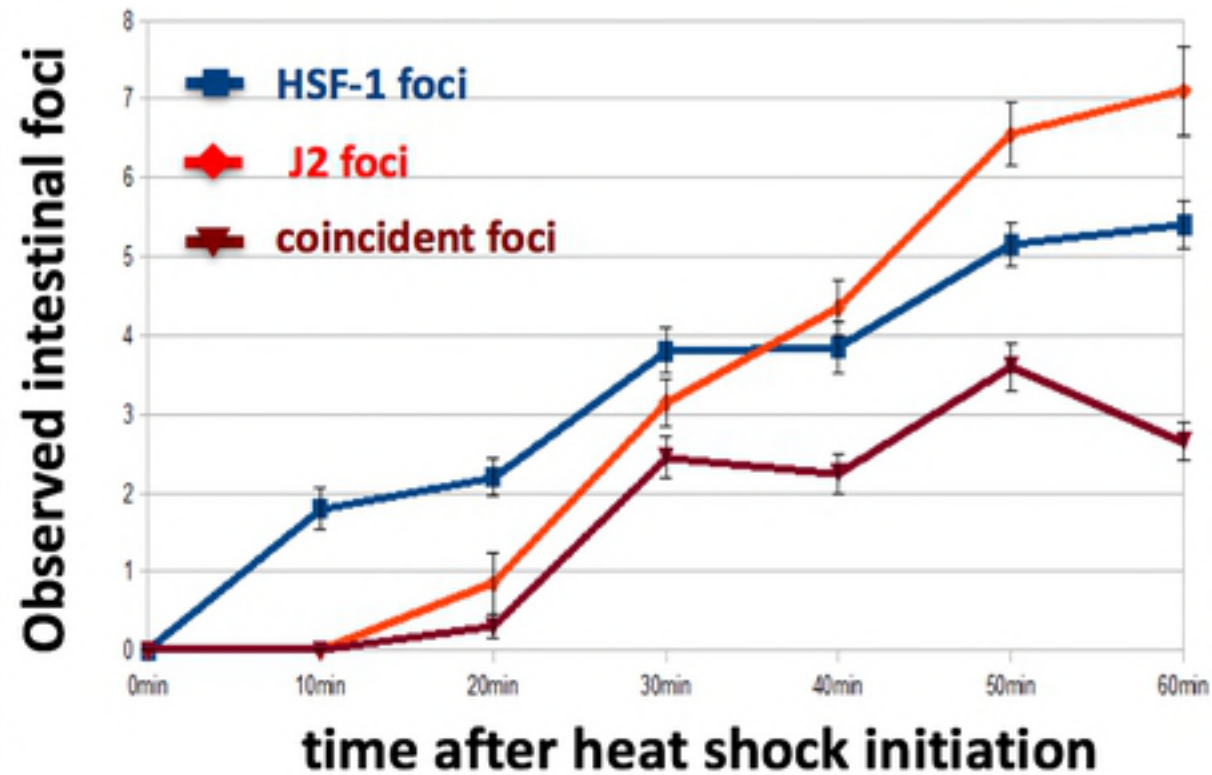
- 559 juggernaut [Internet]. Science. American Association for the Advancement of Science;
560 2016. p. aad9926. doi:10.1126/science.aad9926
- 561 16. Vilborg A, Sabath N, Wiesel Y, Nathans J, Levy-Adam F, Yario TA, et al. Comparative
562 analysis reveals genomic features of stress-induced transcriptional readthrough. *Proc Natl*
563 *Acad Sci*. 2017;114: E8362–E8371. doi:10.1073/pnas.1711120114
- 564 17. Rutkowski AJ, Erhard F, L'Hernault A, Bonfert T, Schilhabel M, Crump C, et al.
565 Widespread disruption of host transcription termination in HSV-1 infection. *Nat Commun*.
566 2015;6. doi:10.1038/ncomms8126
- 567 18. Grosso AR, Leite AP, Carvalho S, Matos MR, Martins FB, Vítor AC, et al. Pervasive
568 transcription read-through promotes aberrant expression of oncogenes and RNA chimeras
569 in renal carcinoma. *Elife*. 2015;4: 1–16. doi:10.7554/eLife.09214
- 570 19. Muniz L, Deb MK, Aguirrebengoa M, Lazorthes S, Trouche D, Nicolas E. Control of
571 Gene Expression in Senescence through Transcriptional Read-Through of Convergent
572 Protein-Coding Genes. *Cell Rep*. ElsevierCompany.; 2017;21: 2433–2446.
573 doi:10.1016/j.celrep.2017.11.006
- 574 20. Wight M, Werner A. Europe PMC Funders Group The functions of natural antisense
575 transcripts. 2015; 91–101. doi:10.1042/bse0540091.The
- 576 21. Saldi TK, Ash PE, Wilson G, Gonzales P, Garrido-Lecca A, Roberts CM, et al. TDP-1,
577 the *Caenorhabditis elegans* ortholog of TDP-43, limits the accumulation of double-
578 stranded RNA. *EMBO J*. 2014;33: 2947–66. doi:10.15252/embj.201488740
- 579 22. Brenner S. The genetics of *Caenorhabditis elegans*. *Genetics*. 1974;77: 71–94.
580 doi:10.1002/cbic.200300625
- 581 23. Porta-de-la-Riva M, Fontrodona L, Villanueva A, Cerón J. Basic *Caenorhabditis elegans*
582 methods: synchronization and observation. *J Vis Exp*. MyJoVE Corporation; 2012; e4019.
583 doi:10.3791/4019
- 584 24. Orjalo A, Johansson HE, Ruth JL. Stellaris fluorescence in situ hybridization (FISH)
585 probes: A powerful tool for mRNA detection. *Nat Methods*. 2011;8: i–ii.
586 doi:10.1038/nmeth.f.349
- 587 25. Thorvaldsdóttir H, Robinson JT, Mesirov JP. Integrative Genomics Viewer (IGV): high-
588 performance genomics data visualization and exploration. *Brief Bioinform*. 2013;14: 178–
589 92. doi:10.1093/bib/bbs017
- 590 26. Andrews S. FastQC: A quality control tool for high throughput sequence data. available
591 from <http://www.bioinformatics.babraham.ac.uk/projects/fastqc/>. 2017; 1.
- 592 27. Bolger AM, Lohse M, Usadel B. Trimmomatic: A flexible trimmer for Illumina sequence
593 data. *Bioinformatics*. Oxford University Press; 2014;30: 2114–2120.
594 doi:10.1093/bioinformatics/btu170
- 595 28. Dobin A, Gingeras TR. Mapping RNA-seq Reads with STAR [Internet]. *Current protocols*
596 *in bioinformatics*. NIH Public Access; 2015. p. 11.14.1–11.14.19.
597 doi:10.1002/0471250953.bi1114s51
- 598 29. Liao Y, Smyth GK, Shi W. FeatureCounts: An efficient general purpose program for
599 assigning sequence reads to genomic features. *Bioinformatics*. 2014;30: 923–930.
600 doi:10.1093/bioinformatics/btt656
- 601 30. Love MI, Huber W, Anders S. Moderated estimation of fold change and dispersion for
602 RNA-seq data with DESeq2. *Genome Biol*. 2014;15: 1–21. doi:10.1186/s13059-014-
603 0550-8
- 604 31. Kaneko H, Dridi S, Tarallo V, Gelfand BD, Fowler BJ, Cho WG, et al. DICER1 deficit

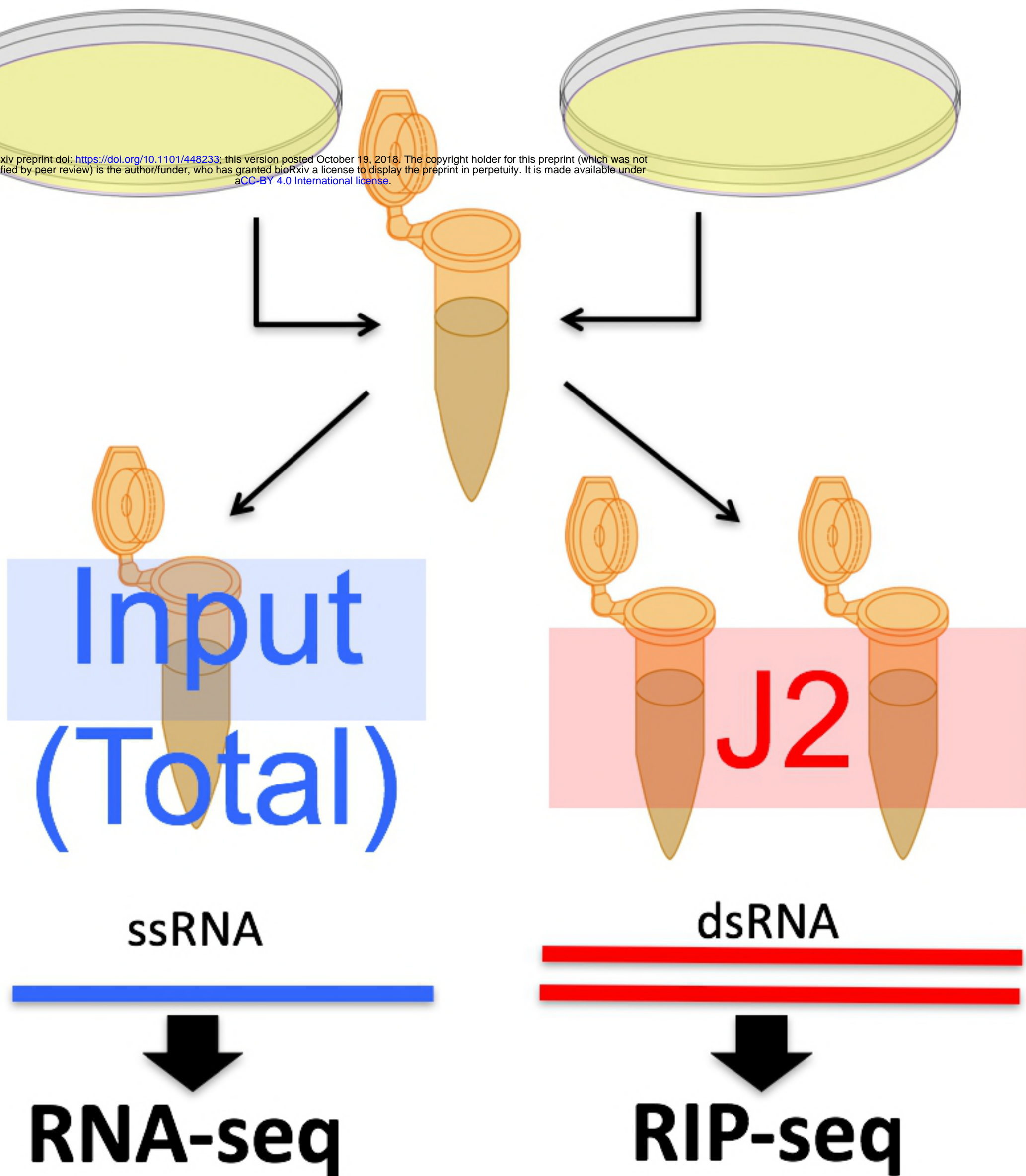
- 605 induces Alu RNA toxicity in age-related macular degeneration. *Nature*. 2011;471: 325–
606 332. doi:10.1038/nature09830
- 607 32. Klopfenstein D V., Zhang L, Pedersen BS, Ramírez F, Warwick Vesztröcy A, Naldi A, et
608 al. GOATOOLS: A Python library for Gene Ontology analyses. *Sci Rep. Nature*
609 Publishing Group; 2018;8: 10872. doi:10.1038/s41598-018-28948-z
- 610 33. Cardiello JF, Goodrich JA, Kugel JF. Heat shock causes a reversible increase in RNA
611 polymerase II occupancy downstream of mRNA genes consistent with a global loss in
612 transcriptional termination. *Mol Cell Biol. American Society for Microbiology Journals*;
613 2018;38: MCB.00181-18. doi:10.1128/MCB.00181-18
- 614 34. Zhang T, Hwang HY, Hao H, Talbot C, Wang J. *Caenorhabditis elegans* RNA-processing
615 protein TDP-1 regulates protein homeostasis and life span. *J Biol Chem*. 2012;287: 8371–
616 8382. doi:10.1074/jbc.M111.311977
- 617 35. Curran SP, Ruvkun G. Lifespan regulation by evolutionarily conserved genes essential for
618 viability. *PLoS Genet*. 2007;3: e56. doi:10.1371/journal.pgen.0030056
- 619
620
621

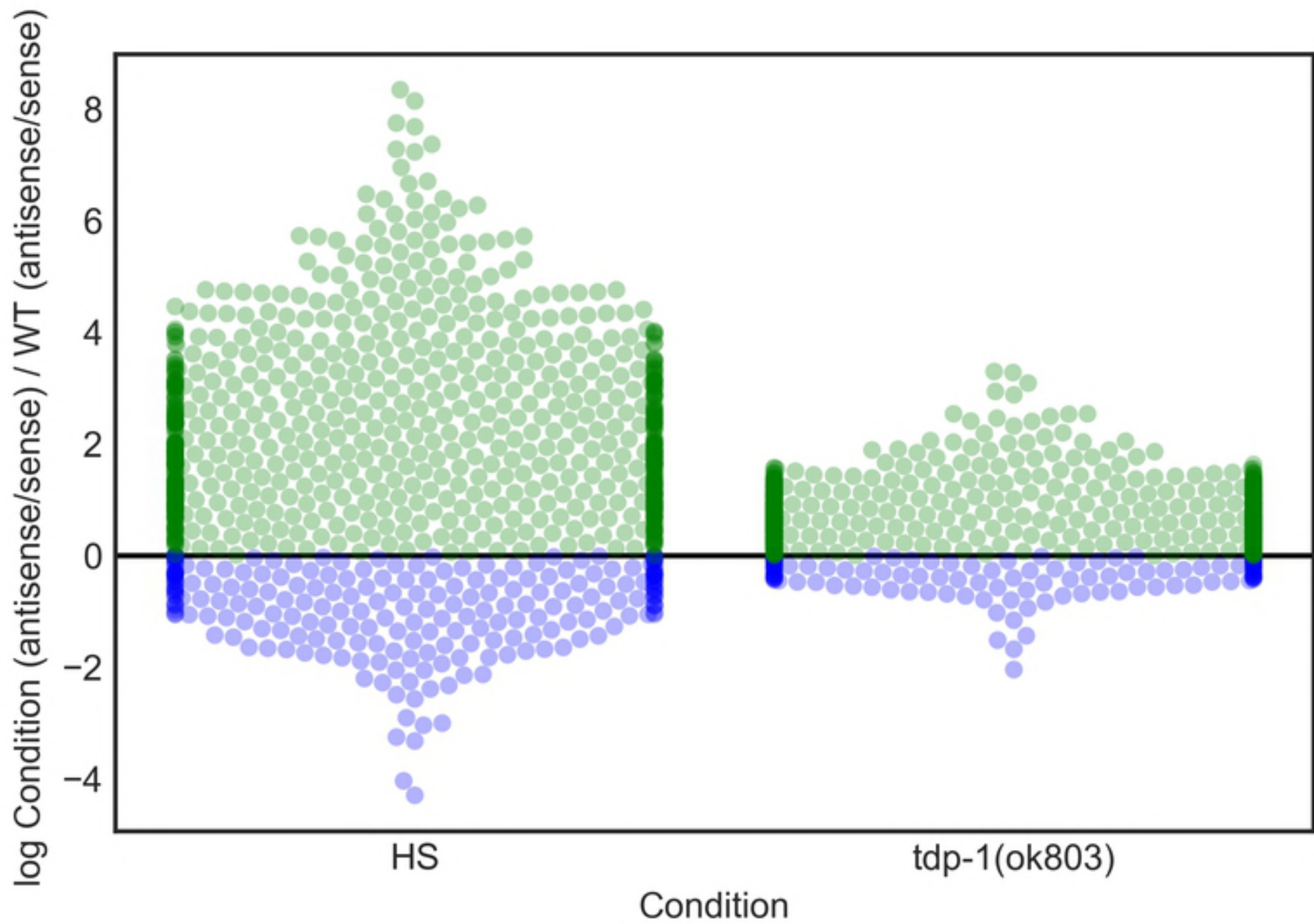
622 **Supporting information**

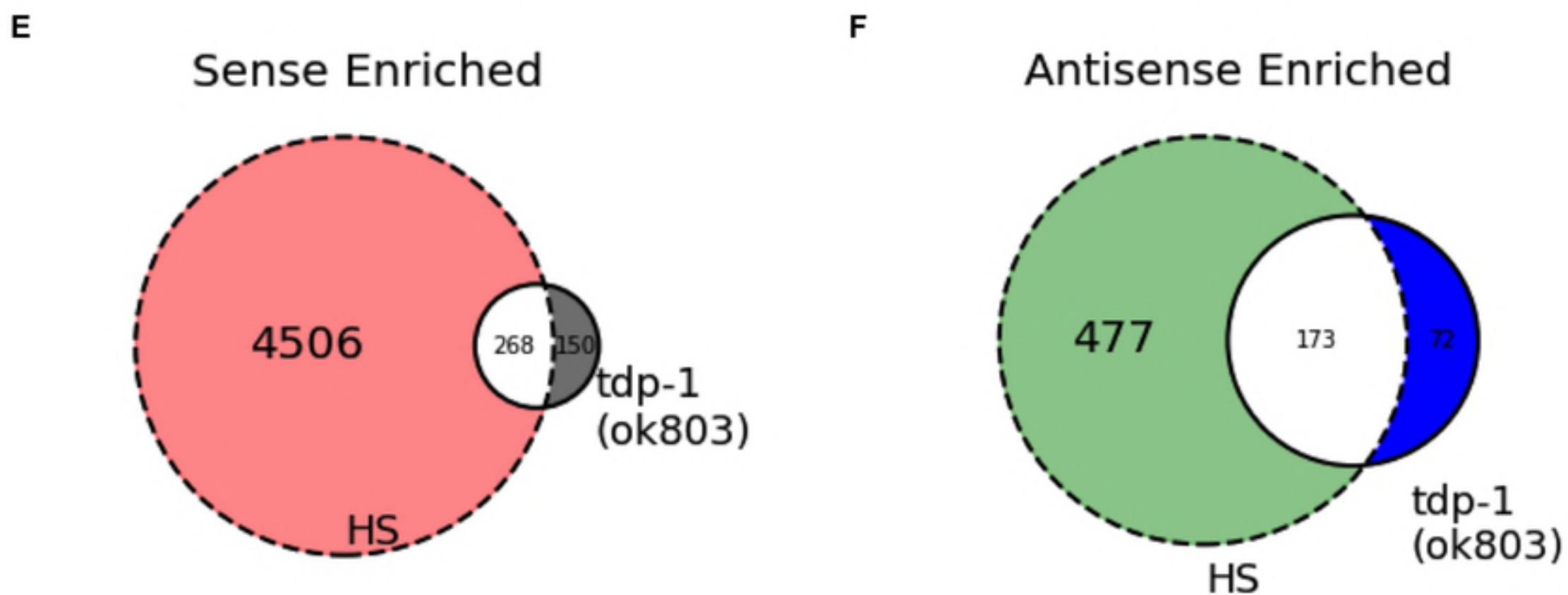
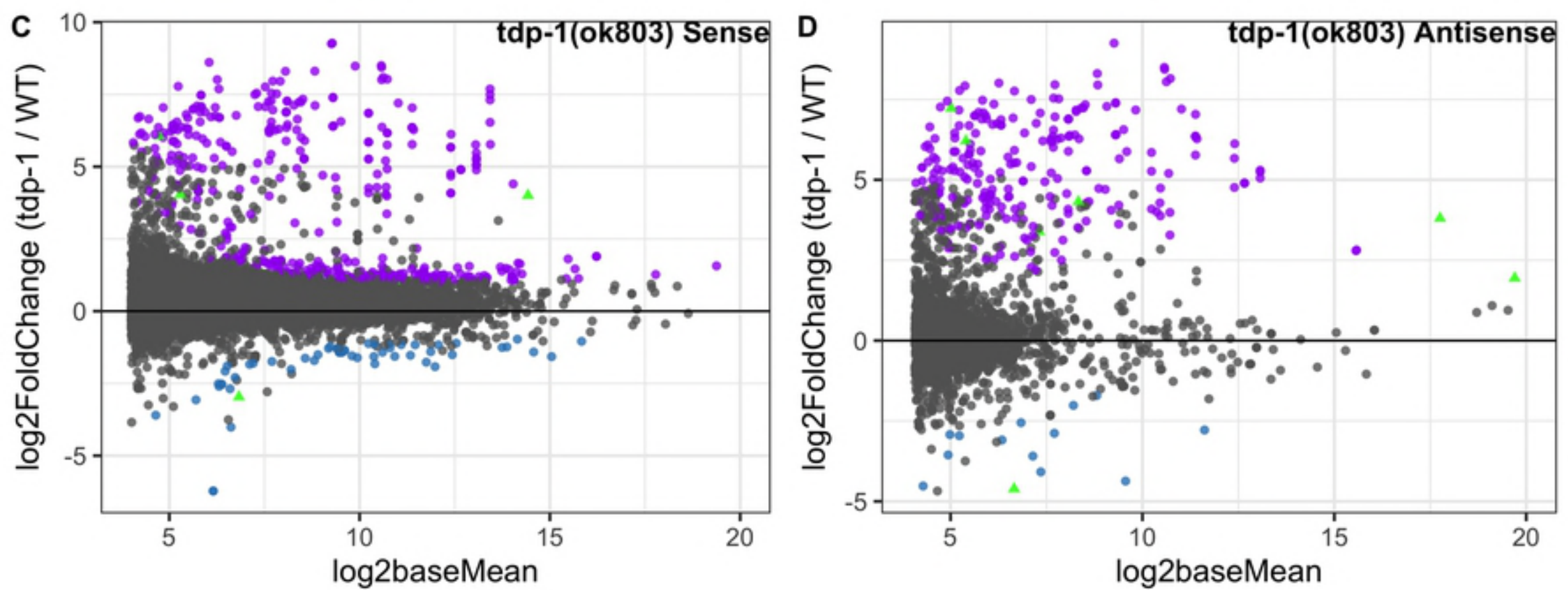
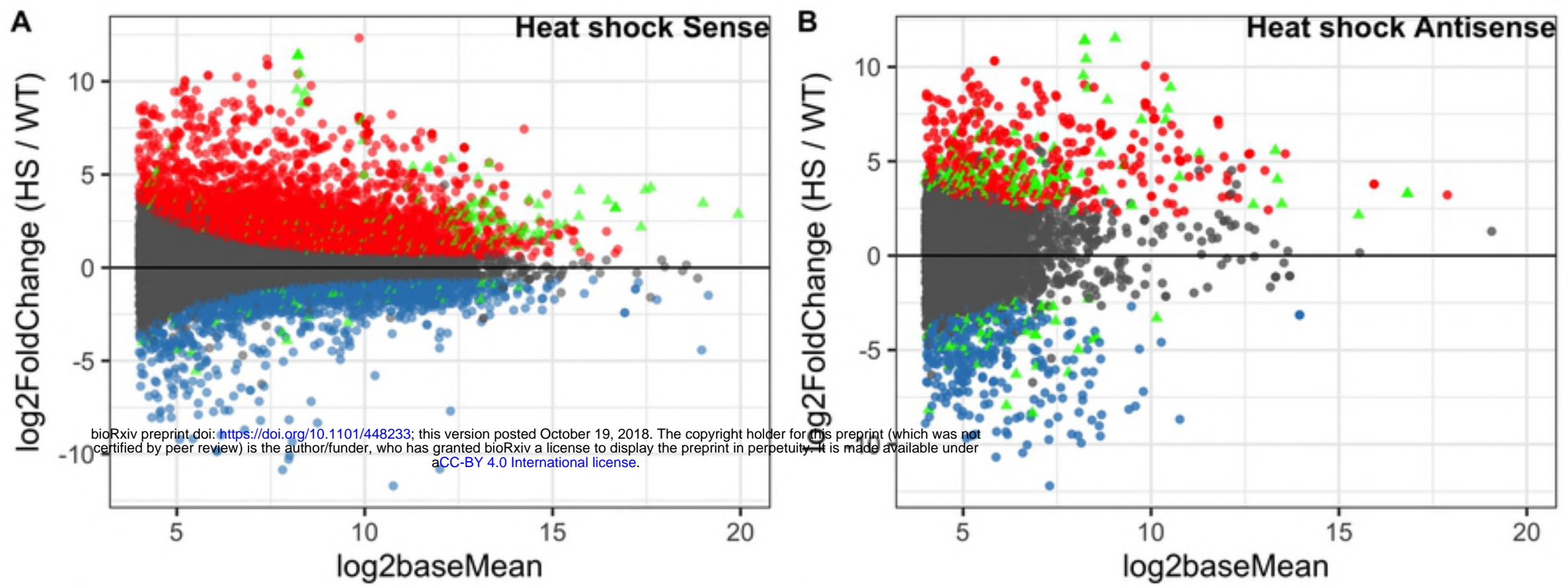
- 623
624 **S1 Fig. Comparison of heat shock J2 enriched transcripts significant in both sense and**
625 **antisense.**
- 626
627 **S1 Table. Worm strains used in this study.**
- 628
629 **S1 File. Probes used in Fluorescence in situ Hybridization (FISH) of eif-3.B regions.**
- 630
631 **S2 Fig. Comparison of *tdp-1(ok803)* J2 enriched transcripts significant in both sense and**
632 **antisense.**
- 633
634 **S2 Table. Quantification of occurrence of HSF-1 and J2 foci over time (Raw data).**
- 635
636 **S3 Fig. Number of Terminal Inverted Repeats (TIR) overlapping downstream regions.**
- 637
638 **S2 File. List and sequences of adapters used in trimming.**
- 639
640 **S3 File. Bioinformatic methods.**
- 641
642 **S4 Fig. Dogcatcher flattening and nomenclature.**
- 643 **S4 File. Hypergeometric Distribution and list of genes/DoGs used in calculation for Heat**
shock and *tdp-1(ok803)*.
- 644
645 **S5 File. List of significant genes, translation associated genes, and overlapped genes.**

- 644 **S5 Fig. Dogcatcher additional filtering.**
645
646 **S6 File. Significantly enriched GO terms for Heat shock and *tdp-1(ok803)* genes.**
- 647 **S6 Fig. Sense and antisense *eif-3B* transcripts do not colocalize.**
648
649 **S7 File. List of significant DoGs, ADoGs, PoGs, APoGs.**
- 650 **S8 File. Significantly enriched GO terms for Heat shock DoGs.**

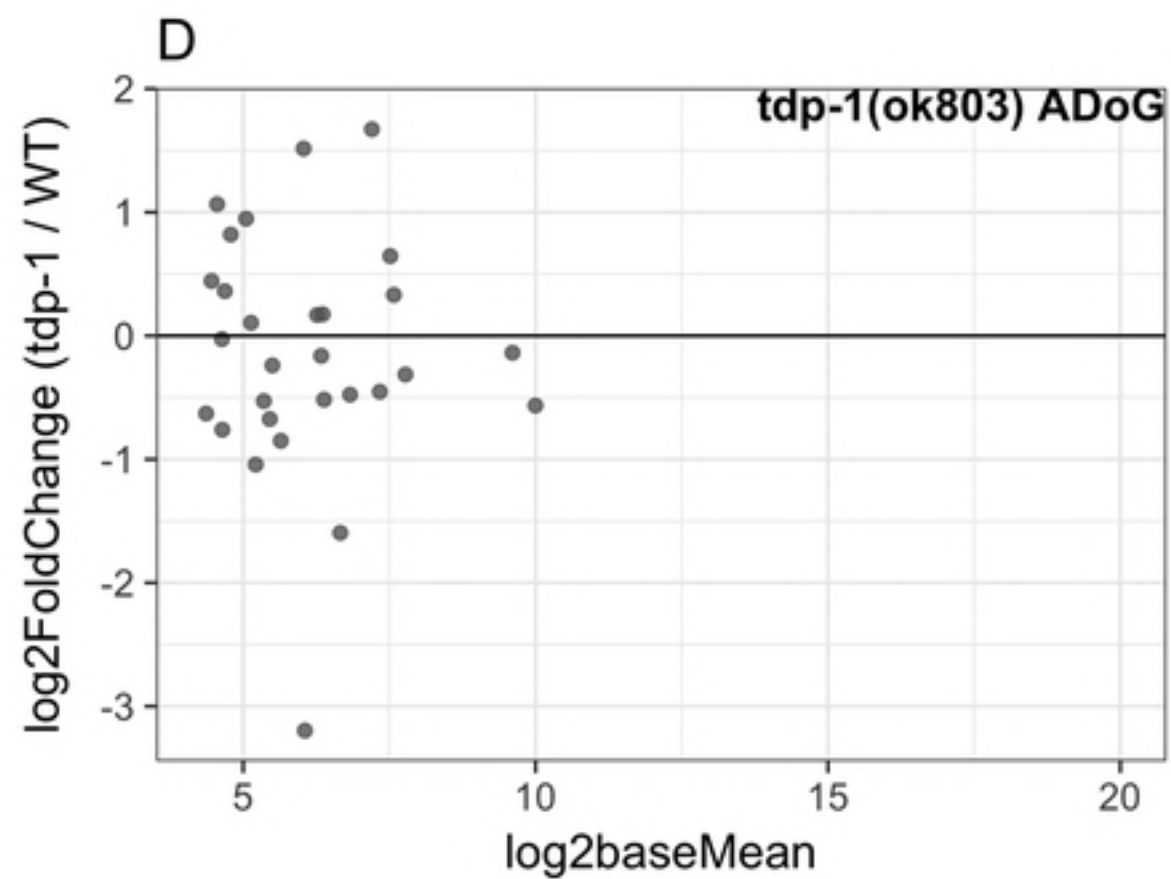
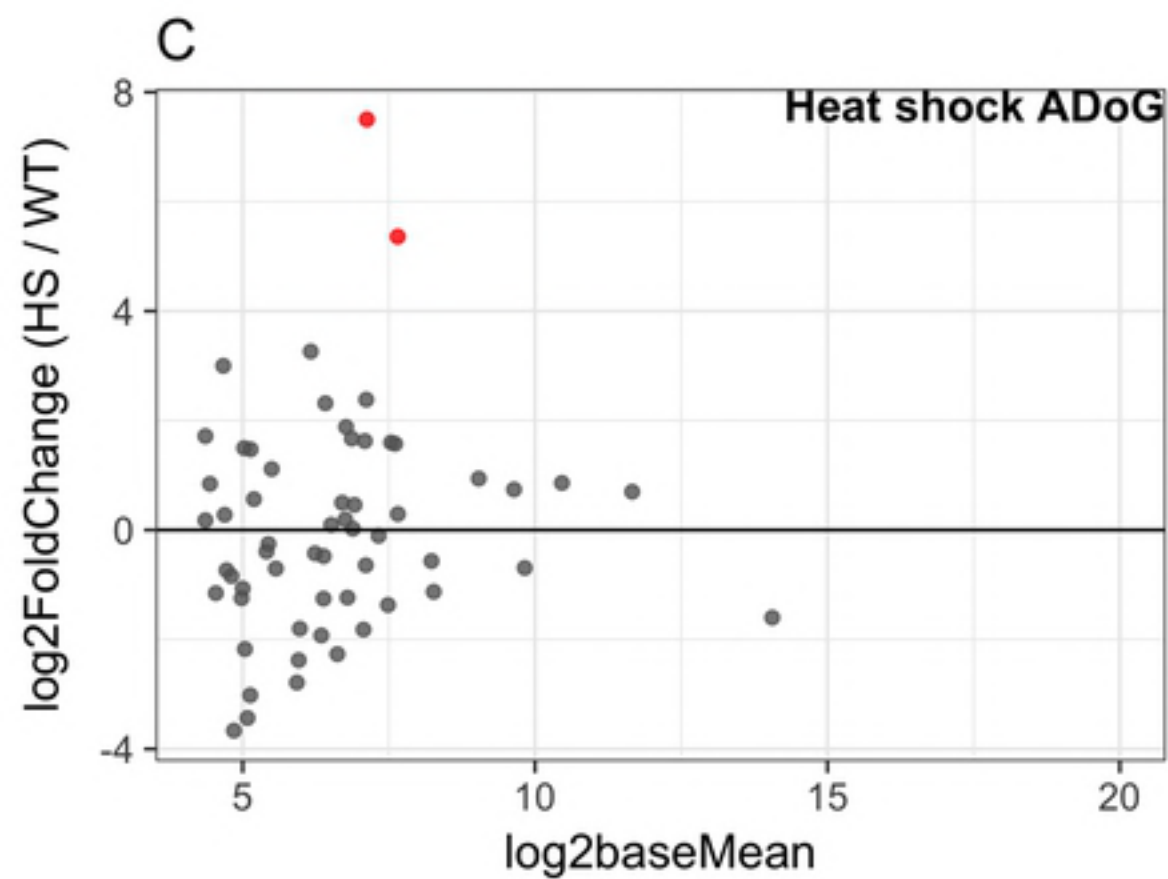
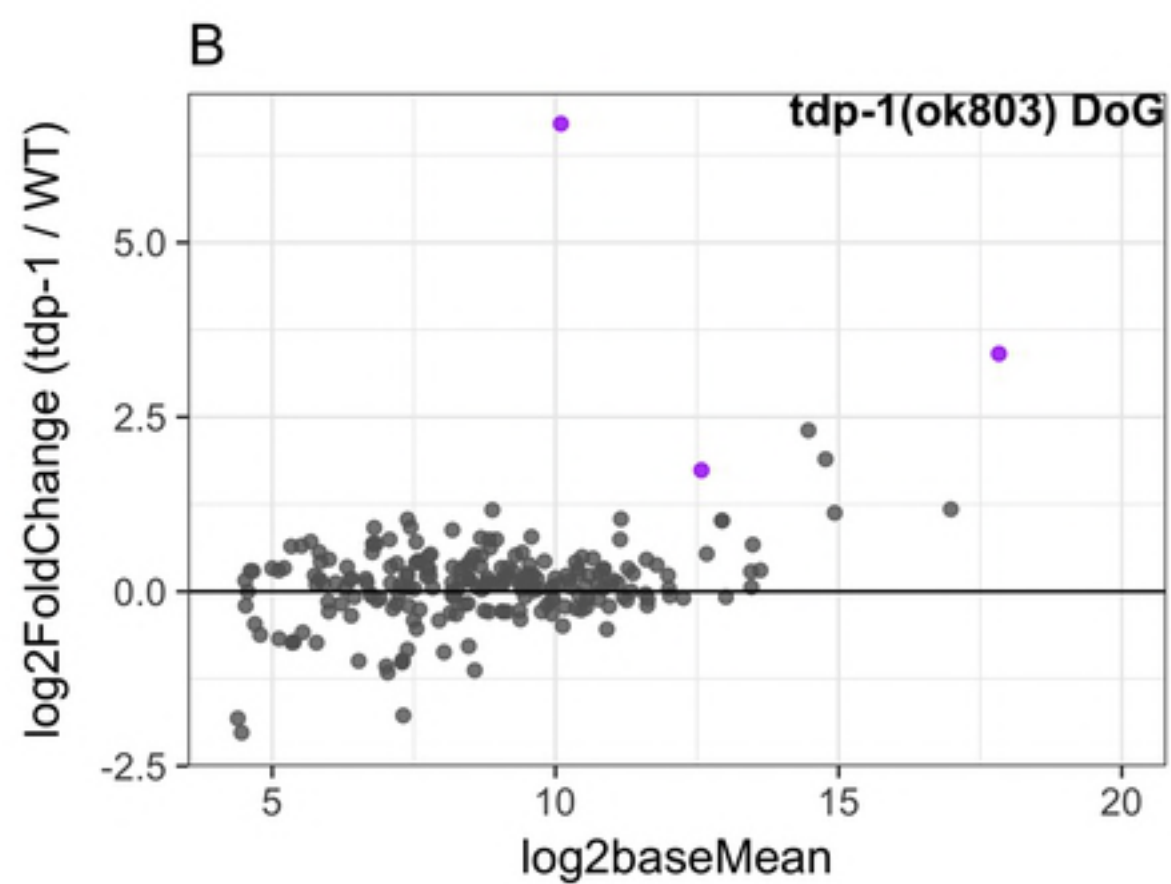
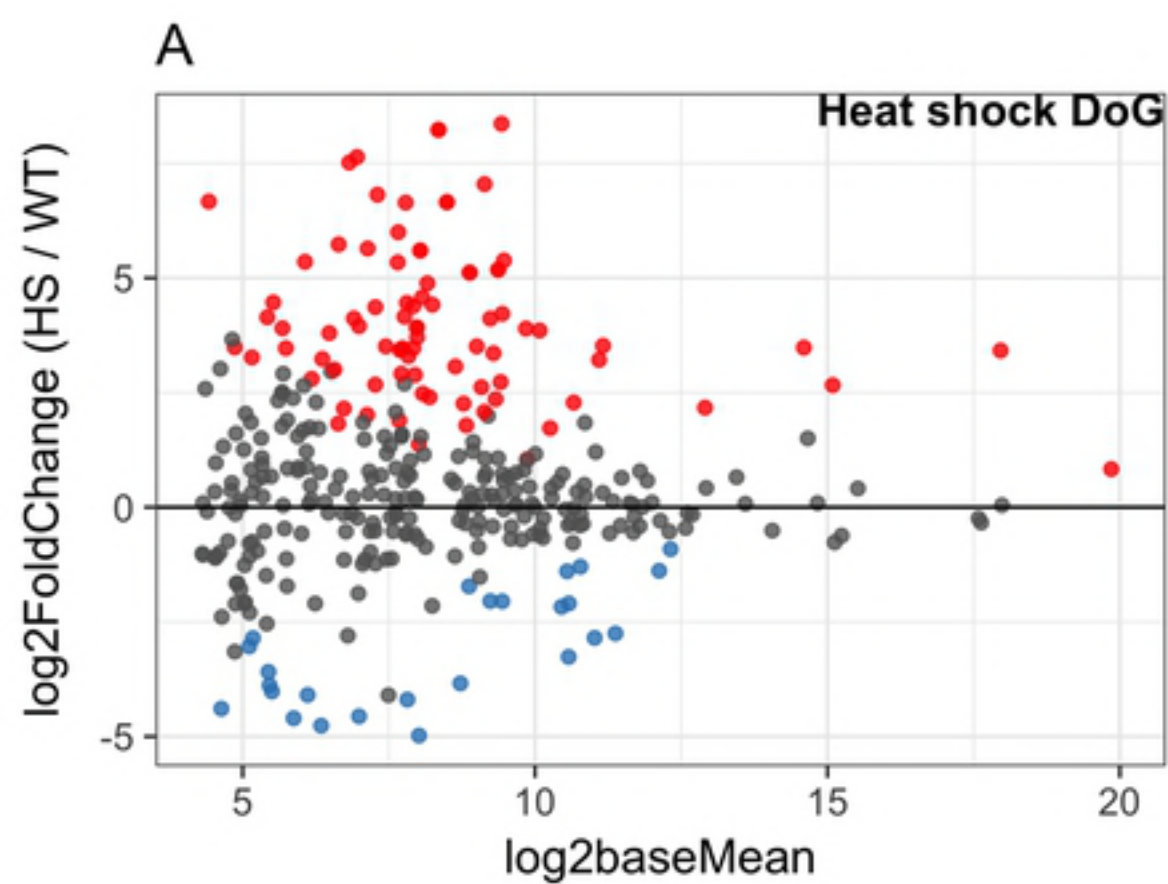
A**B**

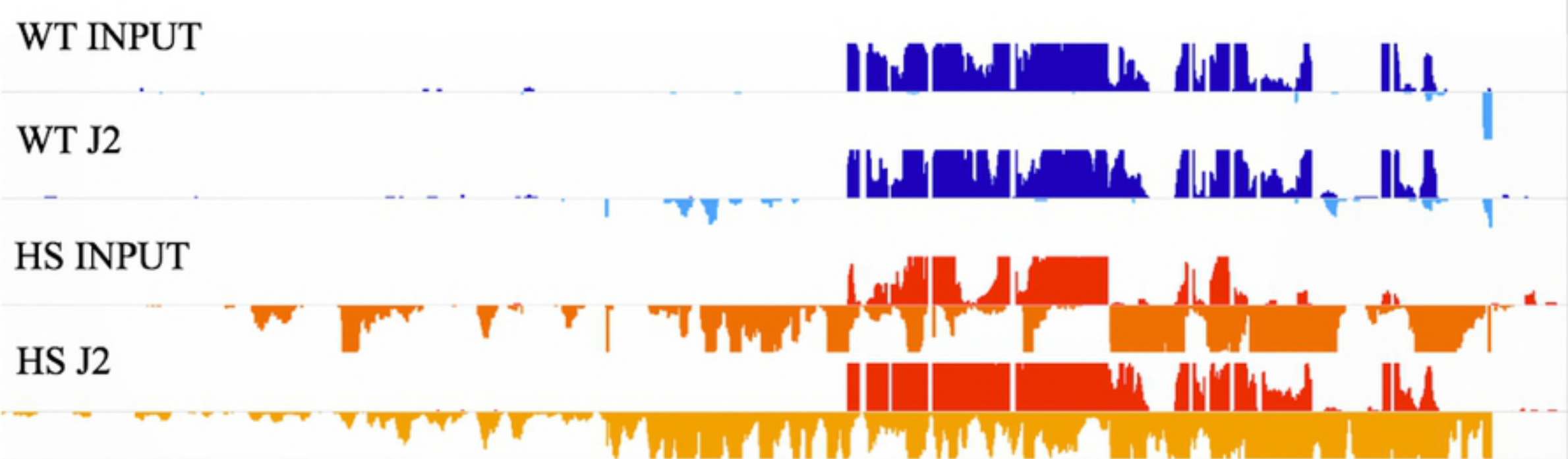








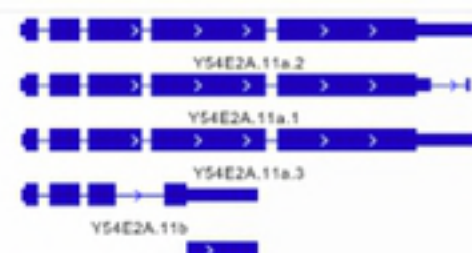




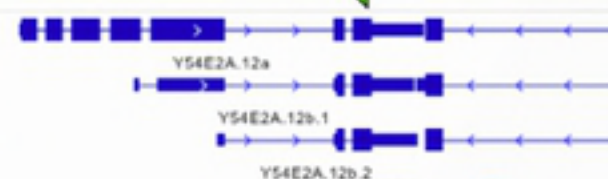
doW01D2.8



WBGene00013195



eif-3.b



tbc-20



5' Intergenic

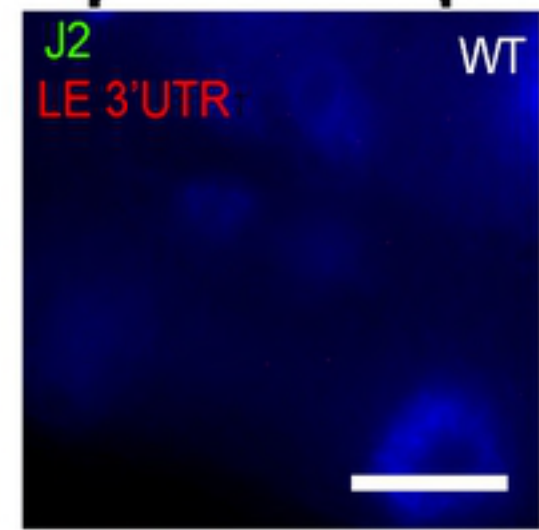
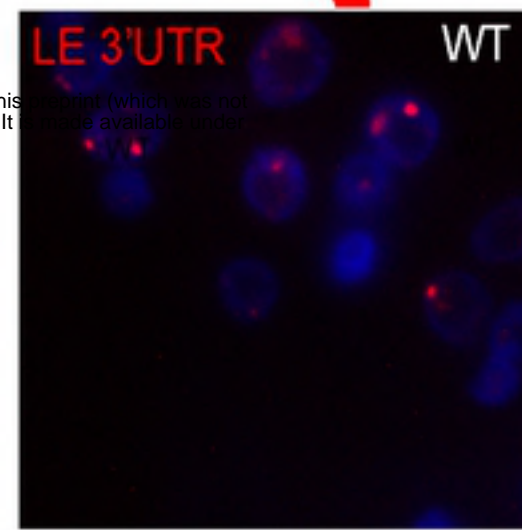
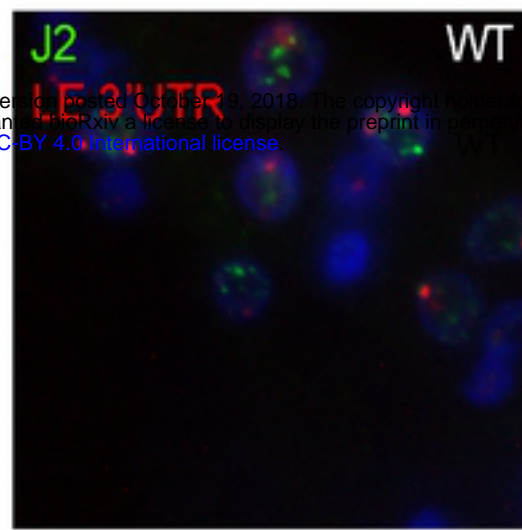
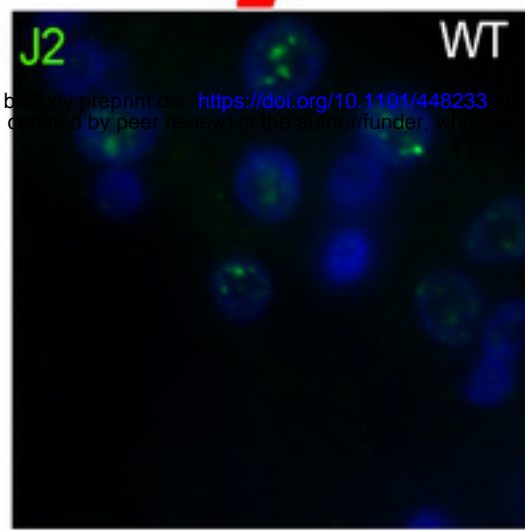
Second Exon

3' UTR

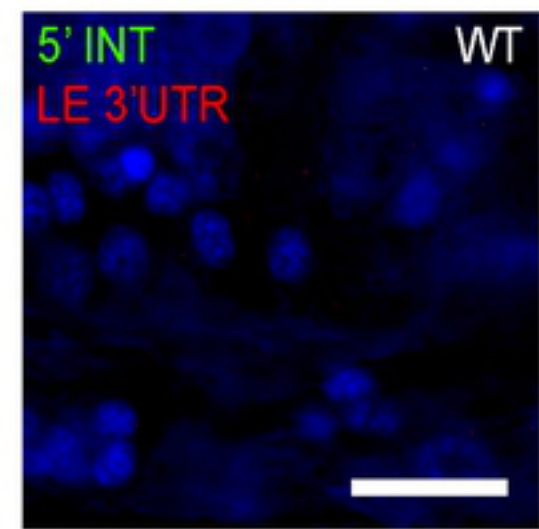
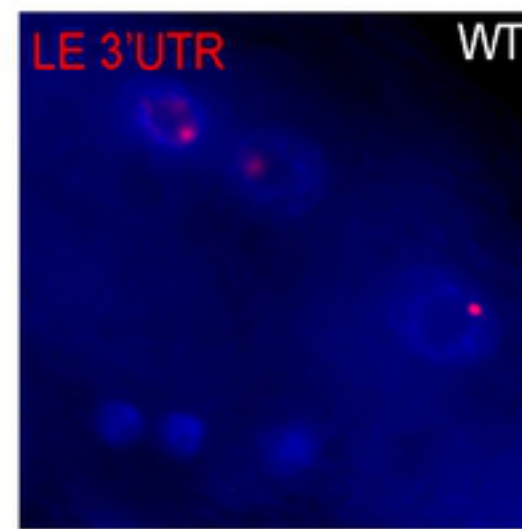
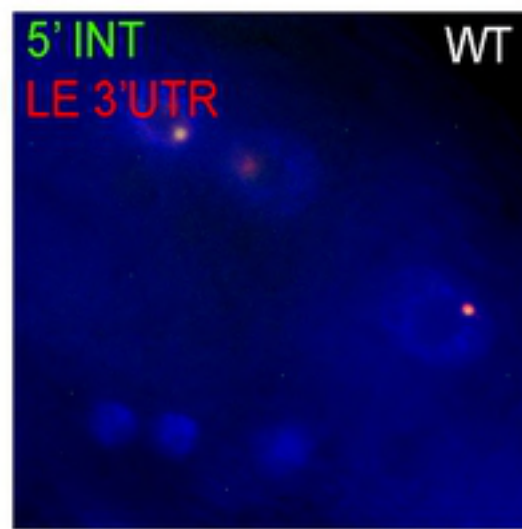
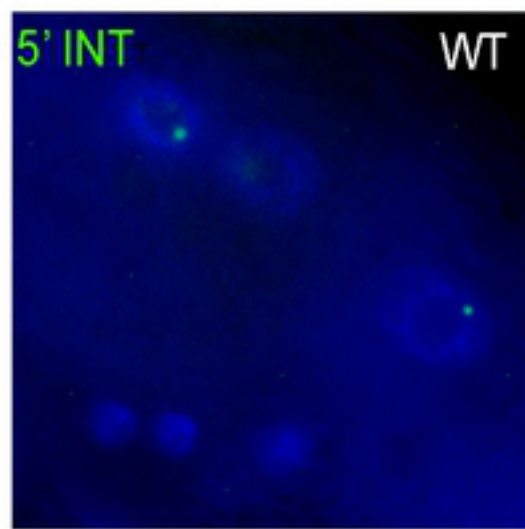
HEATSHOCK

CONTROL

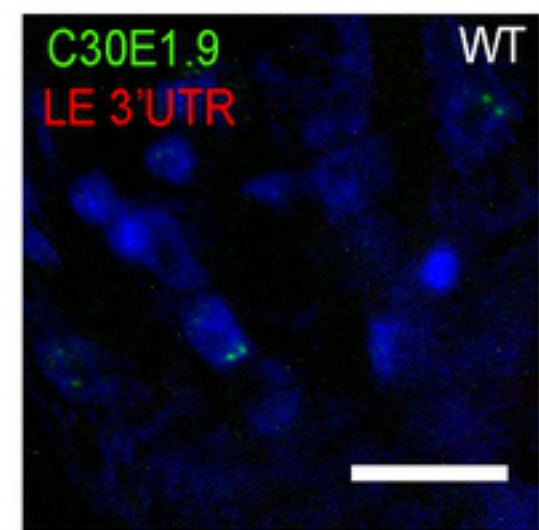
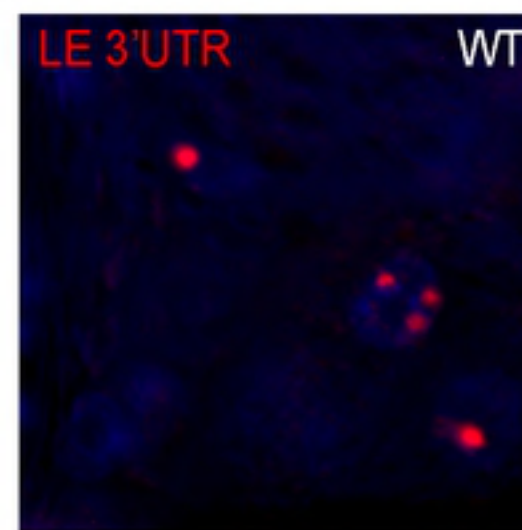
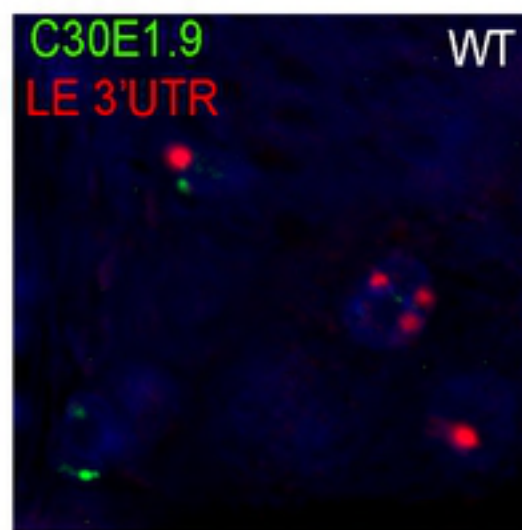
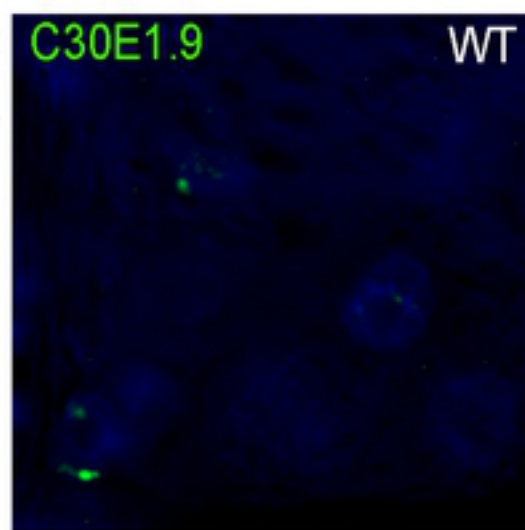
A



B



C



D



E

